*Quantum Electronics* **51** (8) 727–729 (2021) 

https://doi.org/10.1070/QEL17600

# Concept of a miniature photonic spatial switch based on an off-axis zone plate

Yu.E. Geints, O.V. Minin, I.V. Minin

*Abstract.* **A new concept of an all-optical wavelength-selective two-channel switch based on the photonic hook effect without the use of micromechanical devices or nonlinear materials is proposed. A prototype of such a device based on an off-axis Fresnel zone plate is considered and its main parameters are discussed. Due to the unique property of the photonic hook to change its curvature with respect to the irradiation wavelength $\lambda$, this switch is a promising candidate for the implementation of optical switching in modern optoelectronics and miniature 'on-a-chip' devices. Numerical simulation shows that the optical isolation of switched channels for a switch with linear dimensions of about $(6\lambda)^3$ based on an off-axis zone plate can reach 18–20 dB during operation in the wavelength range of 1.5–1.9 μm.**

***Keywords:*** *optical switch, photonic hook, off-axis Fresnel zone plate.*

Optical switching and optical switches are a key element in modern network communications [1]. The requirements for microminiaturisation of devices dictate the need to develop their components and 'on-a-chip' systems of optical type, in contrast to switching circuits based on electronic devices controlled by an external electrical signal [2].

Today, various methods for constructing optical switches are known. Among them, wavelength-selective switches [3–6] have attracted much attention because of their ability to independently route channels with different wavelengths. Usually, optical switches of this type are, in fact, a combination of a diffraction grating spectrometer with a spatial light modulator [1]. A comparison of various types of optical switches was carried out in [7]. Below, we propose a new concept of a wavelength-selective, all-optical switch based on recently discovered structured spatially localised light beams, called a 'photonic hook' [8, 9]. This concept allows the implementation of a nonmechanical and all-optical 'on-a-chip' switch that changes the direction of the output radiation without the use of nonlinear materials [10].

The physical principle, on the basis of which we propose to implement contactless spectral-selective switching of optical channels, relies on the effect of generating a curved photon flux when an optical wave propagates through a specific diffractive optical element with dimensions of the order of the wavelength. In principle, a curved photon flux (photonic hook) can be formed in several ways. One of them is to use an optically homogeneous particle having a geometric asymmetry or an asymmetry of the illuminating beam. For example, it can be a rectangular prism, a cylinder [11, 12] or an ellipsoid under lateral illumination [13], an asymmetric planar lens in the form of a mesowave off-axis phase plate [14], etc. Another method for obtaining a curved photon flux uses geometrically symmetric particles with a specially formed refractive index asymmetry [11]. These are the so-called Janus particles obtained by combining two or more materials with different optical characteristics [15].

An important property of a photonic hook for implementing the function of an optical switch is the dependence of the angle of curvature of its arms on the irradiation wavelength. Therefore, with a certain spatial configuration of the photonic microstructure and reception zones, it is possible to achieve a change in the magnitude of the optical signal in each of the channels when the radiation wavelength changes.

The considered type of the asymmetric photonic structure in the form of an off-axis binary Fresnel phase plate (PP) used in numerical simulation is shown in Fig. 1. The PP consisted of seven phase zones etched in a glass substrate with a refractive index $n = 1.5$, and was calculated for a telecommunication wavelength $\lambda = 1550$ nm and a focal length $f = 15$ μm at a zone etching depth of about $\lambda$ to obtain the maximum intensity at the focus [16]. The spatial tilt of the near-field focusing region was ensured by using a circular diaphragm with a diameter of 6 μm, which was placed outside the optical axis of the plate and, therefore, opened up an asymmetric configuration of Fresnel zones for operation. With such geometrical parameters of the mesoscale PP, the dimensional Mie parameter is $q = 2\pi r/\lambda = 3.87\pi$ ($r$ is the PP radius), which corresponds to the condition for the existence of the photonic jet effect [17, 18].

The computer simulation of the optical switch was performed on the basis of the numerical solution of Maxwell's differential equations for field vectors in three-dimensional spatial geometry, implemented in the Lumerical software package (version 8). The PP was placed inside a three-dimensional grid region that was located in the air (refractive index $n_0 = 1$) and surrounded by a system of perfectly matched layers (PMLs) to implement free radiation conditions at the external boundaries of the computational domain. A plane optical wave illuminating the plate propagated in the direction of the wave vector $\boldsymbol{k}$ along the normal to the substrate with an optical switch and had an initial amplitude of 1 V m$^{-1}$

**Yu.E. Geints** V.E. Zuev Institute of Atmospheric Optics, Siberian Branch, Russian Academy of Sciences, pl. Akad. Zueva 1, 634055 Tomsk, Russia;
**O.V. Minin, I.V. Minin** Siberian State University of Geosystems and Technologies, ul. Plakhotnogo 10, 630108 Novosibirsk, Russia; National Research Tomsk Polytechnic University, prosp. Lenina 30, 634050 Tomsk, Russia; e-mail: prof.minin@gmail.com

Received 7 June 2021
*Kvantovaya Elektronika* **51** (8) 727–729 (2021)
Translated by M.A. Monastyrskiy

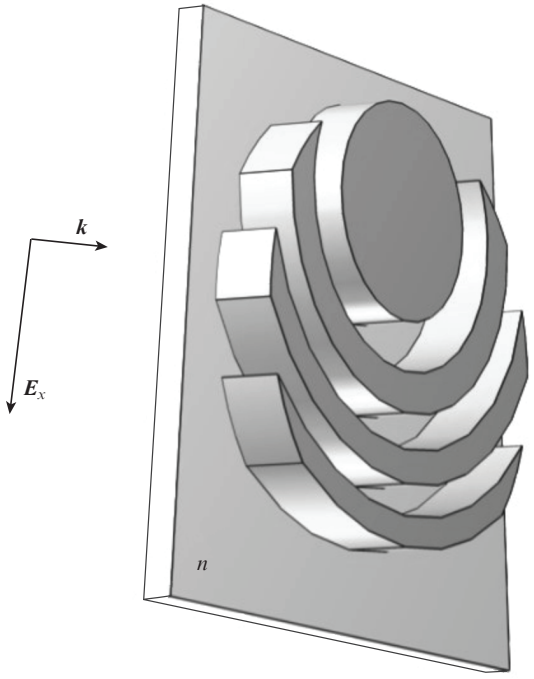


**Figure 1.** Off-axis PP on a quartz substrate.

and a linear polarisation of the field $\boldsymbol{E}$ along the $x$ axis. To discretise the computational domain, an adaptive spatial grid with minimum and maximum steps of 0.5 and 50 nm, respectively, was used, providing automatic refinement of the grid cells in areas with a large dielectric constant gradient. The time step of the numerical scheme in accordance with the Courant condition was 0.25 fs. In this case, the total number of Yee cells throughout the simulated space was equal to ~15 million.

Figure 2 shows a two-dimensional distribution of the squared amplitude (intensity) of a plane optical wave $|\boldsymbol{E}|^2$ diffracted on the PP. It can be seen that the angle $\gamma$ of the beam deflection, which arises behind the particle of a curved localised electromagnetic field (photonic hook), depends on the incident radiation wavelength $\lambda$. The placement of two optical receivers, P1 and P2, in the plane $z = 20$ μm provides different field amplitudes in each channel when operating at different wavelengths, i.e., their spatial switching according to the optical signal level. It is obvious that the operation reliability of such a switch is determined by the value of the optical isolation of the channels, which, in turn, depends on the parameters of the switching microparticle and the range of irradiation wavelengths.

Note that to improve the optical isolation of the switched channels, it is necessary to adjust the input aperture of the receiving ports in accordance with the cross-section of the photonic jet. In the case of mesowave [17] PPs, the characteristic diameter of the photonic jet measured at the point of maximum intensity has the order of the radiation wavelength [17, 18]. During propagation (due to diffraction), the jet size increases; therefore, in our studies, the diameter of the receiving aperture of the ports was assumed to be equal to 2 μm. Subsequently, the optical field energy entering the receiving ports can be accumulated by a miniature photodetector based, for example, on a plasmon antenna [19, 20], and analysed by any discriminator scheme that compares signals from two ports.

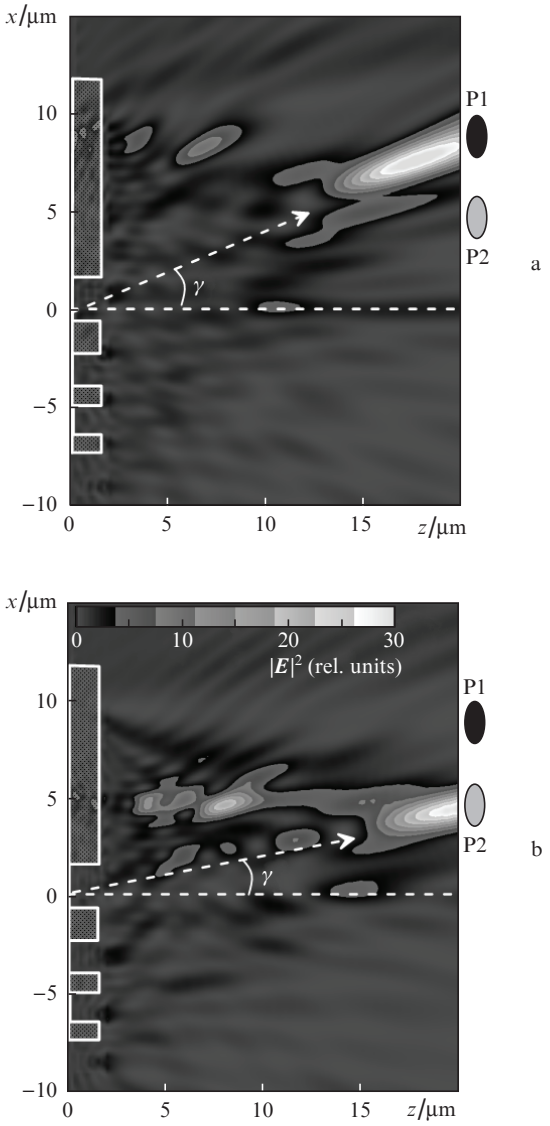


**Figure 2.** Intensity profiles of the optical field $|\boldsymbol{E}|^2$ for plane wave diffraction with (a) $\lambda_1 = 1.31$ μm and (b) $\lambda_2 = 1.8$ μm on an off-axis PP.

The result of such a comparison in the form of a logarithm of the ratio of the energies $W_1$ and $W_2$ that entered the receiving ports is shown in Fig. 3b. Here is the dependence of the relative energy transmission $S = \lg(W_1/W_2)$ on the irradiation wavelength, where the energies $W_{1,2}$ are the integral of the field intensity over the cross-sectional area $\Sigma$ of the corresponding receiving port:

$$W_{1,2} = \int_{\Sigma_{1,2}} |E|^2 \mathrm{d}\boldsymbol{\sigma}.$$

The absolute extremes on these curves can be attributed to the alternative states of the photon switch, when the signal $S_1$ from the first port (P1 in Fig. 3a) or the signal $S_2$ from the second port (P2) prevails. In Fig. 3b, such states are marked with large circles. The signal difference $\Delta S = S_1 - S_2$ can serve as a measure of the optical isolation (decoupling) of switching channels.

It can be seen that the optical isolation coefficient $\Delta S$ can reach 20 dB, and this is a good indicator, provided that the switch is triggered almost instantly. Thus, the spectral range

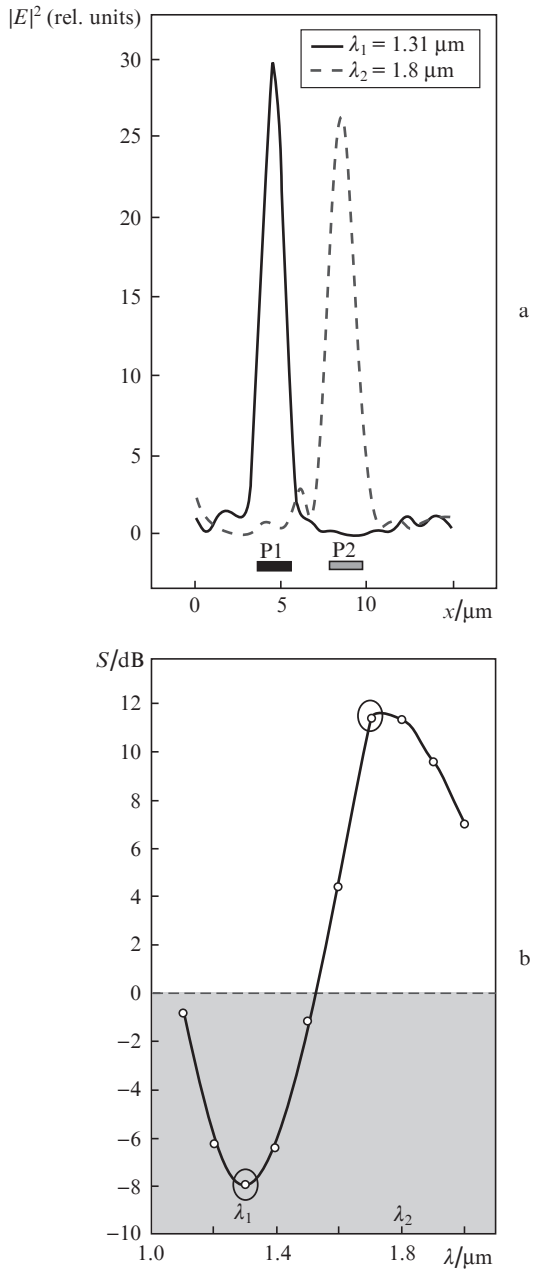


**Figure 3.** (a) Transverse optical intensity profiles in the plane $z = 20$ μm in the vicinity of ports at different switching wavelengths and (b) relative energy transmission $S$ of receiving ports versus the irradiation wavelength of the off-axis PP.

in which the switching of states is realised is about 500 nm. It should be noted that under conditions when $\Delta S \approx 0$, the photonic switch under discussion begins to function as an optical splitter, since the field energy in both channels is equalised. However, due to the 'open' nature of the type of optical switching under consideration, the energy loss for splitting will be quite large.

Note that instead of a wavelength-selective optical switch, it is possible to use switching the spatial orientation of the photonic hook by changing the polarisation of the incident radiation, as was demonstrated, for example, in works [11, 13], but the discussion of this type of optical switches is beyond the scope of this paper.

Thus, we have shown the fundamental possibility of developing an all-optical two-channel miniature (with a size of the order of the wavelength) switch (photonic hook) based on a dielectric microstructure with a broken geometric shape symmetry, made in the form of an off-axis PP. Due to the unique property of the photonic hook to change the angle of its bending with respect to the irradiation wavelength and at the same time maintain an extreme spatial localisation at distances several times greater than the Rayleigh diffraction length [8, 9, 11–13, 17], this switch is a good candidate for the implementation of optical switching in modern optoelectronics and miniature 'on-a-chip' devices without the use of micromechanical systems or nonlinear materials and in the absence of electrical signal control, as in works [21–23].

***Acknowledgements.*** This work was performed within the framework of the TPU development programme and partially supported by the Russian Foundation for Basic Research (Grant No. 21-57-10001) and the Ministry of Science and Higher Education of the Russian Federation (V. E. Zuev Institute of Atmospheric Optics of the Russian Academy of Sciences).

## References

1. El-Bawab T.S. *Optical Switching* (Boston, MA: Springer, 2006).
2. Stabile R., Albores-Mejia A., Rohit A., et al. *Microsyst. Nanoeng.*, **2**, 15042 (2016).
3. Seok T.J., Luo J., Huang Z., Kwon K., Henriksson J., Jacobs J., Ochikubo L., Muller R.S., Wu M.C. *APL Photonics*, **4**, 100803 (2019).
4. Han S., Seok T.J., Quack N., Yoo B.W., Wu M.C. *Optica*, **2**, 370 (2015).
5. Strasser T.A., Wagener J.L. *IEEE J. Sel. Top. Quantum Electron.*, **16**, 1150 (2010).
6. Zhang C., Zhang M., Xie Y., Shi Y., Kumar R., Panepucci R., Dai D. *Photonics Res.*, **8**, 1171 (2020).
7. Singh O., Paulus R. *Opt. Commun.* (2021); https://doi.org/10.1515/joc-2020-0284.
8. Dholakia K., Bruce G.D. *Nat. Photonics*, **13**, 225 (2019).
9. Christodoulides D.N., in *The Photonic Hook* (Cham: Springer, 2021) pp vii,viii. DOI:10.1007/978-3-030-66945-4.
10. Notomi M., Tanabe T., Shinya A., Kuramochi E., Taniyama H. *Adv. Opt. Technol.*, ID 568936 (2008). DOI:10.1155/2008/568936.
11. Geints Y., Minin I.V., Minin O.V. *J. Opt.*, **22**, 065606 (2020).
12. Minin I.V., Minin O.V., Liu C., Wei H., Geints Y., Karabchevsky A. *Opt. Lett.*, **45** (17), 4899 (2020).
13. Liu C., Chung H., Minin O.V., Minin I.V. *J. Opt.*, **22** (8), 085002 (2020).
14. Minin I.V., Minin O.V., Golodnikov D.O. *Proc. 8th Int. Conf. on Actual Problems of Electronic Instrument Engineering* (Novosibirsk, Russia, 2006) pp 13–18. DOI:10.1109/APEIE.2006.4292375.
15. Su H., Hurd Price H., Jing L., Tian Q., Liu J., Qian K. *Mater. Today Bio*, **4**, 100033 (2019).
16. Ali S., Jacobsen C. *J. Opt. Soc. Am. A*, **37** (3), 374 (2020).
17. Minin I.V., Minin O.V., Geints Y.E. *Ann. Phys. (Berlin)*, **527** (7-8), 491 (2015).
18. Littlefield A., Zhu J., Messinger J.F., Goddard L.L. *Optics & Photonics News*, **32** (1), 34 (2021).
19. Tang L., Kocabas S., Latif S., Okyay A.K., Ly-Gagnon D., Saraswat K.C., Miller D.A.B. *Nat. Photonics*, **2**, 226 (2008).
20. Dorodnyy A., Salamin Y., Ma P., Plestina J., Lassaline N., Mikulik D., Romero-Gomez P., Morral A., Leuthold J. *IEEE J. Sel. Top. Quantum Electron.*, **24** (6), 4600313 (2018).
21. Plander I., Stepanovsky M. *Open Comput. Sci.*, **6**, 116 (2016).
22. Li M., Liang H., Luo R., He Y., Ling J., Lin Q. *Optica*, **6**, 860 (2019).
23. Jia S., Peng J., Bian J., Zhang S., Xu S., Zhang B. *Micromachines*, **12**, 221 (2021).